Optimizing Vehicle and Pedestrian Trade-Off Using Signal Timing in Intersections with Center Transit Lanes

Jing Zhao, Ph.D.[1]; and Wanjing Ma, Ph.D.[2]

Abstract: The construction of exclusive bus lanes is a strategy for giving priority to buses and improving the efficiency of the urban transportation system, and for that purpose, center transit lanes are an important type of transit lane. Along the center transit lanes, the operation of intersections with bus stops becomes more complex because there are four kinds of travelers that need to be organized: buses, private vehicles, crossing pedestrians, and bus passengers. This paper presents a signal timing model for intersections with center transit lanes and bus stops to balance the trade-off between the operations of various users. The optimization model is formulated as a two-objective programming problem. In each subobjective, the weighted average person delay is used. The Pareto frontier of solutions is obtained by iterating all possible combinations of weights for the two objectives. For each combination of weights, the optimization problem becomes a single-objective programming problem. The performance of the proposed model is evaluated using a case study and extensive numerical analyses. A shorter cycle length is recommended to balance the trade-off between vehicles and pedestrians. For the geometric design, a near-side bus stop and larger central refuge island are recommended. **DOI: 10.1061/JTEPBS.0000145.**

Author keywords: Signal timing; Intersections; Center transit lane; Vehicle and pedestrian delay; Pareto optimization.

Introduction

With the continued growth of urban roadway congestion, many cities throughout the world are choosing to construct exclusive bus lanes on their road networks that give priority to buses in order to build a more efficient transportation system (Chen et al. 2009; Diakaki et al. 2015; Khoo et al. 2014). These exclusive bus lanes could be built in many ways, including center, offset, curbside, and contraflow transit lanes. Center transit lanes are typically used on major routes with frequent headways and where traffic congestion may significantly affect reliability (NACTO 2016). The bus stop is one of the most important facilities in this bus system. For center transit lanes, boarding islands must be placed in the street, and they are usually located at intersections for the convenience of passengers. The operation of the intersection becomes more complex because it includes four kinds of travelers: buses, private vehicles, crossing pedestrians, and bus passengers. If they are not properly organized, the operational order and efficiency will be seriously disturbed.

The optimal geometric design and control of intersections has long been a concern for the researchers. A large number of studies have focused on the vehicles. One of the traditional treatments is to add more approach lanes or turning pockets provided there is available space at the intersection (El Esawey and Sayed 2013). An alternative solution is to optimize the signal control, which includes two general approaches: (1) the stage-based method (Allsop 1971; Webster 1958), and (2) the group-based method (Heydecker and Dudgeon 1987; Improta and Cantarella 1984; Silcock 1997). In recent years, the optimization of the geometric design and signal timings was combined using a lane-based model to achieve the best operational performance of the intersection and relieve traffic congestion (Wong and Wong 2003a, b; Wong and Heydecker 2011). Moreover, traffic-flow uncertainty is taken into consideration (Cascetta et al. 2006; Szeto and Lo 2005; Yin 2008). To adapt the time-varying characteristics of traffic flow in the real world, robust signal optimization and online (adaptive) signal control have been proposed. For robust optimization, the signal parameters are predetermined based on historical data to maintain satisfactory performance under flow fluctuations (Yin 2008; Zhang et al. 2010). For online optimization, the signal parameters are dynamically adjusted based on real-time traffic measurements and prediction of future demand (Liu et al. 2015; Tong et al. 2015).

Although prior research has sought many designs to enhance capacity, it has been unable to address the continued growth of vehicular demand. Therefore, researchers have suggested providing public transport with priority to speed up transit vehicles and improve the overall system efficiency (Diakaki et al. 2015; TRB 2013). Constructing exclusive bus lanes is a common strategy for enhancing the performance of bus transit (Chen et al. 2009; Khoo et al. 2014). The idea of exclusive bus lanes was first introduced (Ma et al. 2014a; Yu et al. 2015) in the 1930s. Up to now, extensive numerical and empirical studies have been conducted for optimizing the construction of exclusive bus lanes. At the macroscopic level, researchers have performed several investigations for determining the road in which a lane should be reserved as an exclusive bus lane (Khoo et al. 2014). Exclusive bus lane allocation, traffic assignment, transit assignment, modal split, and bus line scheduling have been combined to expand the effects of exclusive bus lanes at the road-network level (Abdelghany et al. 2007; Khoo et al. 2014; Kim and Suh 1988; Li and Ju 2009; Mesbah et al. 2011a, b; Miandoabchi et al. 2012; Yao et al. 2012; Yu et al. 2015). At the microscopic level, the geometric design of exclusive bus lanes has been carefully discussed. Exclusive bus lanes could be center,

[1]Associate Professor, Dept. of Traffic Engineering, Univ. of Shanghai for Science and Technology, 516 Jungong Rd., Shanghai 200093, P.R. China (corresponding author). E-mail: jing_zhao_traffic@163.com

[2]Professor, Key Laboratory of Road and Traffic Engineering of the Ministry of Education, Tongji Univ., 4800 Cao'an Rd., Shanghai 201804, P.R. China. E-mail: mawanjing@tongji.edu.cn

Note. This manuscript was submitted on July 20, 2017; approved on December 12, 2017; published online on April 10, 2018. Discussion period open until September 10, 2018; separate discussions must be submitted for individual papers. This paper is part of the ***Journal of Transportation Engineering, Part A: Systems***, © ASCE, ISSN 2473-2907.

offset, curbside, or contraflow transit lanes (NACTO 2016). Among these types of exclusive bus lanes, the center lane can play a key role in creating a high-quality transit service (NACTO 2016). It could offer significant benefits from dedicated infrastructure for reducing the chance of conflict with turning movements, illegal parking along the roadway edge, and cyclists.

To further ensure transit priority, transit-signal priority (TSP) was proposed at intersections with exclusive bus lanes (Duerr 2000; Janos and Furth 2002; Lin 2002), involving three main types of priority strategy: passive, active, and real-time (Balke et al. 2000; Furth and Muller 2000; Ma et al. 2010, 2013; Skabardonis 2000). TSP produces different effects on the different types of exclusive bus lanes (Xu and Zheng 2012). Particularly, for center transit lanes, to avoid conflicts between left-turn vehicles and center-running transit vehicles, adequate signal timing is essential. Kim (2010) proposed a triple-ring phase representation scheme to harmonize the nonbus and exclusive bus phases. The proposed model could increase the average travel speed and the throughput of nonbus through movements by assigning residual time to the nonbus phases on the exclusive median bus lane corridors. However, in all TSP strategies, it is assumed that the lane assignment of both the exclusive bus lanes and private vehicle lanes are provided as exogenous inputs. It is difficult to determine an optimal set of lane markings with the corresponding transit priority. To remedy this deficiency, Ma et al. (2014a) developed a person-capacity-based optimization method for the integrated design of lane markings, exclusive bus lanes, and passive bus priority signal settings for isolated intersections. Two traffic modes, namely passenger cars and buses, were considered in the unified framework.

Besides the vehicles, pedestrian traffic is also an important mode. Balancing the needs of pedestrians and vehicles is a critical problem at signalized intersections. Initially, the signal timing of pedestrians is considered by imposing constraints such as a minimum green time requirement and pedestrian clearance time (TRB 2010). Then, to remedy the issue of the fixed design of the pedestrian clearance interval (PCI), a fuzzy-logic control-based signal control system was developed for an isolated intersection with the concept of dynamic PCI (Lu et al. 2011). To further increase the level of service to the pedestrian, optimal control models with objectives to minimize the pedestrian delay were proposed by using a microsimulation model (Ishaque and Noland 2005) and genetic algorithm (GA) optimization procedure (Yang and Benekohal 2011). The factors considered include the influence of pedestrian-vehicle conflict (Fitzpatrick 2007; Guo et al. 2004; Wei et al. 2015), pedestrian arrival rate (Chilukuri and Virkler 2005; Griffiths et al. 1985; Kruszyna et al. 2006), signal noncompliance (Li et al. 2005; Nagraj and Vedagiri 2013; Virkler 1998; Ye et al. 2015), two-stage crossing (Ma et al. 2011; Wang and Tian 2010), and bidirectional pedestrian flow (Goh and Lam 2004; Lee and Lam 2008). Moreover, to increase the ease and convenience in pedestrian crossing around a downtown area, an exclusive pedestrian phase was proposed. Pedestrians are allowed to cross the intersection in all directions (including diagonally and laterally) at the same time during the exclusive pedestrian phase (Bechtel et al. 2004; Kattan et al. 2009).

A multiobjective optimization model for the optimization of the pedestrian-phase patterns was proposed, including an exclusive pedestrian phase and conventional two-way crossing (Ma et al. 2014b). The optimal pedestrian-phase pattern and signal timings at an intersection to accommodate vehicle and pedestrian movements were determined. The model was further extended to be an economic evaluation framework to establish quantitative criteria for the phase selection for pedestrians with both safety and efficiency factors considered (Ma et al. 2015). Recently, optimization of pedestrian signal timings was also incorporated into the lane-based signal optimization model (Yu et al. 2017). Both vehicle and pedestrian traffic were integrated into a unified framework for the optimization of isolated intersections with one-stage and two-stage crosswalks. The total weighted delay of pedestrians and vehicles was adopted as the objective function, and temporal and spatial constraints were explicitly formulated.

Although much is known about the geometric and signal timing design of intersections, the optimization design of intersections with center transit lane stops has rarely been discussed. Because none of the studies mentioned earlier considered the four kinds of travelers, namely private vehicles, buses, pedestrians, and passengers, in a unified optimization model, some new conditions need to be dealt with in this paper:

- Trade-offs between the efficiency of vehicle traffic (including private vehicles and buses) and pedestrian traffic (including crossing pedestrians and passengers at the bus stop);
- Limitations of the central refuge island waiting area for accommodating crossing pedestrians and alighting passengers; and
- Effects of the location of center transit lane stops (near side and far side) on the operational efficiency of vehicles and pedestrians.

This paper aims to develop an optimal signal control model to address these critical issues.

Problem Description

A four-leg intersection with center transit lane and stops is illustrated in Fig. 1. Without loss of generality, the center transit lane is set on the east–west road. The bus stops can be set at the near side or far side of the approach. The crosswalk can have one stage or two stages. The optimization problem is conducting the optimal signal timing design of intersections considering the operational efficiency of four kinds of travelers, namely private vehicles, buses, pedestrians, and bus passengers. Pedestrians are the people who will not board or alight from the bus. Bus passengers are those who do board or alight. Because the boarding islands are placed in the center of the street for center transit lanes, bus passengers must cross half of the crosswalk. To facilitate the model presentation, the notations used hereafter are summarized in the "Notation" section.

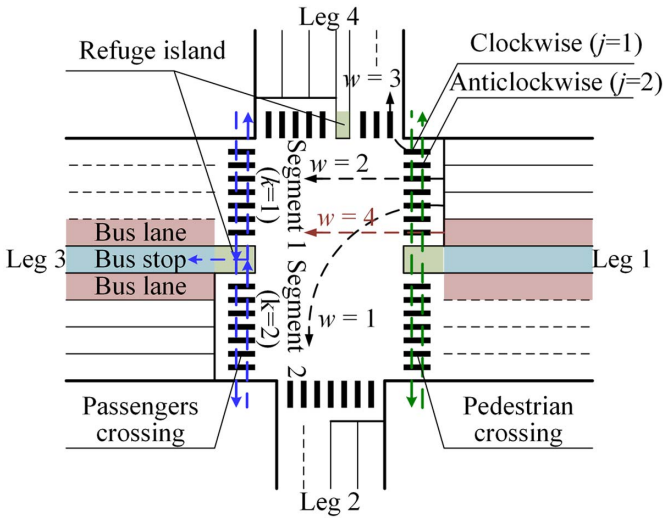

Fig. 1. Four-leg intersection with center transit lane stops

Optimization Model

To balance the trade-off between operations of vehicles and pedestrians, an optimization model is developed with the two conflicting objectives: (1) minimizing the weighted average delay of all vehicular movements, including private vehicles and buses; and (2) minimizing the weighted average delay of pedestrians, including crossing pedestrians and boarding and alighting passengers. Five groups of constraints are considered, including (1) person volume of vehicles (i.e., the product of the volume of vehicles and average number of passengers in vehicles), (2) phase plan of the vehicles, (3) phase plan of the pedestrians, (4) limitations of the signal timing parameters, and (5) limitations of the central refuge island waiting area.

Objective Function

The purpose of this paper is to maximize the operational efficiency of the intersection, which contains two main groups of travelers: vehicles and pedestrians. Therefore, two conflicting objectives are considered. One is minimizing the weighted average delay of all vehicular movements, which includes private vehicles and buses. The other is minimizing the weighted average delay of pedestrians, which includes crossing pedestrians and passengers from the bus stops. The objective function could be given by

$$\min D^v \tag{1}$$

$$\min D^p \tag{2}$$

The vehicles involve private vehicles and buses. The weighted average delay of the vehicles can be calculated by Eq. (3). To reflect the effect of the high occupancy of buses, the person volume is used as the weight for each movement

$$D^v = \frac{\sum_{i\in\mathcal{L}}\sum_{w\in\mathcal{T}} Q_{iw}^v d_{iw}^v}{\sum_{i\in\mathcal{L}}\sum_{w\in\mathcal{T}} Q_{iw}^v} \tag{3}$$

The pedestrian traffic contains the crossing pedestrians as well as boarding and alighting passengers. The weighted average delay of pedestrians can be calculated by Eq. (4)

$$D^p = \frac{\sum_{i\in\mathcal{L}}\sum_{j\in\mathcal{J}} Q_{ij}^{pe} d_{ij}^{pe}}{\sum_{i\in\mathcal{L}}\sum_{j\in\mathcal{J}} Q_{ij}^{pe}} + \frac{\sum_{i\in\mathcal{L}}\sum_{j\in\mathcal{J}} Q_{ijk}^{pa} d_{ijk}^{pa}}{\sum_{i\in\mathcal{L}}\sum_{j\in\mathcal{J}} Q_{ijk}^{pa}} \tag{4}$$

The vehicle delay is calculated by the following formula, which is based on random arrivals and regular departure patterns. It contains the control delay and incremental delay in the delay model of Highway Capacity Manual (HCM) (TRB 2010)

$$d_{iw}^v = \frac{0.5C\left(1-\frac{g_{iw}^v}{C}\right)^2}{1-\left[\min\left(1,\frac{q_{iw}^v C}{s_{iw}^v g_{iw}^v}\right)\frac{g_{iw}^v}{C}\right]} + 900T\left[\frac{q_{iw}^v C}{s_{iw}^v g_{iw}^v} - 1 + \sqrt{\left(\frac{q_{iw}^v C}{s_{iw}^v g_{iw}^v}-1\right)^2 + \frac{4q_{iw}^v C^2}{(s_{iw}^v g_{iw}^v)^2 T}}\right];$$
$$\forall\ i \in \mathcal{L}; \qquad w \in \mathcal{T} \tag{5}$$

The pedestrian delay model should consider three cases: (1) delay model for one-stage crosswalk of pedestrians on the street; (2) delay model for two-stage crosswalk pedestrians on the street; and (3) delay model of passengers of the center transit lane stops.

The crossing pedestrian delay of the one-stage crosswalk can be calculated as the shaded area in Fig. 2(a), as shown in Eq. (6) (TRB 2010)

$$d_{ij}^{pe1} = \frac{(C-g_{ij}^p)^2}{2C}; \quad \forall\ i \in \mathcal{L}; \qquad j \in \mathcal{J} \tag{6}$$

For the two-stage crosswalk design, the pedestrian delay in the first-stage crossing can be calculated as a one-stage crossing delay because of the randomness of the pedestrian arrivals. However, the pedestrian arrivals of the second-stage crossing are related to the first-stage signal. Pedestrians who arrive during the flashing do not walk (FDW) and stop intervals of the first-stage crossing will cross the street simultaneously as a group. However, the pedestrians who arrive at the intersection during the walk time (green time) of the first-stage crossing will have different delays for the second-stage crossing because they do not arrive at the median as a group (Wang and Tian 2010).

The signal coordination between first-stage and second-stage crossings can be categorized into four types, as illustrated in Fig. 3. The pedestrians who cross the first-stage crosswalk at the beginning of the green may arrive at the median refuge island after (Types 1 and 2) or before the start of green of the second-stage crosswalk (Types 3 and 4). Moreover, pedestrians who cross the first-stage crosswalk at the end of the green may arrive at the median refuge island before (Types 1 and 3) or after the start of green of the second-stage crosswalk (Types 2 and 4). According to the relationship between the signal timing of the first-stage and second-stage crossings, the pedestrian delay of the second-stage crossing can be calculated as the shaded area in Figs. 2(b–e), as shown in Eq. (7). Then, the pedestrian delay of the two-stage crosswalk can be calculated by adding the delay on first stage and second stage crosswalks, as shown in Eq. (8)

$$\begin{aligned}
&d_{ij}^{pe\,s} = 0, t_{ij}^b < t_{ij}^w; \qquad t_{ij}^e > t_{ij}^w \\
&\frac{1}{2C}(t_{ij}^w - t_{ij}^e)(2C - 2g_{ijj}^p - t_{ij}^w + t_{ij}^e), \qquad t_{ij}^b < t_{ij}^w; \qquad t_{ij}^e < t_{ij}^w \\
&\frac{1}{2C}(t_{ij}^b - t_{ij}^w)(2C - 2g_{ij(3-j)}^p + t_{ij}^b - t_{ij}^w), \qquad t_{ij}^b > t_{ij}^w; \qquad t_{ij}^e > t_{ij}^w \\
&\frac{1}{2C}[(t_{ij}^w - t_{ij}^e)(2C - 2g_{ijj}^p - t_{ij}^w + t_{ij}^e) + (t_{ij}^b - t_{ij}^w)(2C - 2g_{ij(3-j)}^p + t_{ij}^b - t_{ij}^w)], \qquad t_{ij}^b > t_{ij}^w; \qquad t_{ij}^e > t_{ij}^w
\end{aligned} \tag{7}$$

$$d_{ij}^{pe2} = d_{ij}^{pe1} + d_{ij}^{pe\,s}; \quad \forall i \in \mathcal{L}; \qquad j \in \mathcal{J} \tag{8}$$

J. Transp. Eng., Part A: Systems, 2018, 144(6): 04018023

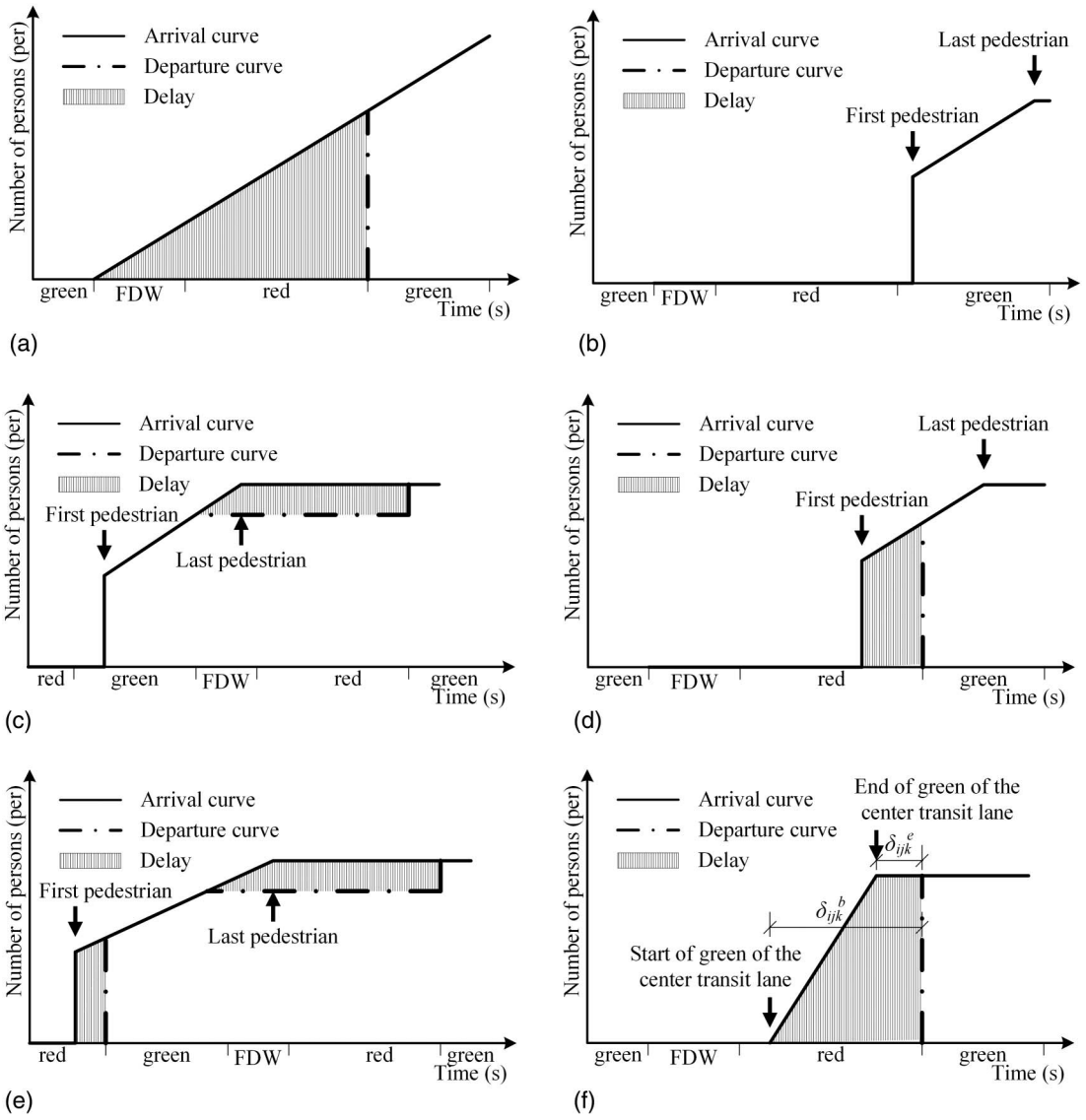

Fig. 2. Calculation diagrams for pedestrian delay model: (a) one-stage crosswalk; (b) second stage (Type 1); (c) second stage (Type 2); (d) second stage (Type 3); (e) second stage (Type 4); (f) far-side bus stop

The passengers at the center transit lane bus stop will board and alight the buses from the median. They must cross half of the crosswalk. The boarding passengers arrive randomly. Therefore, the delay for the boarding passengers can be calculated as a one-stage crossing delay. For the alighting passengers, if the bus stop is located at the near side of the intersection, the passengers arrive randomly; if the bus stop is located at the far side of the intersection, the passengers arrive during the green time of the center transit lane. The delay of passengers can be calculated as the shaded area in Figs. 2(a and f) for the near-side and far-side bus stops, respectively. The delay model of the passengers of the center transit lane stop is shown in Eq. (9)

$$d_{ijk}^{pa} = \begin{cases} \dfrac{(C-g_{ijk}^{p})^2}{2C}, & \forall\ i \in \mathcal{L}; \quad j+k=3 \\ \dfrac{(C-g_{ijk}^{p})^2}{2C}, & \forall\ i \in \mathcal{L}; \quad j+k \neq 3; \quad \beta = 1 \\ \dfrac{\delta_{ijk}^{b}+\delta_{ijk}^{e}}{2} & \forall\ i \in \mathcal{L}; \quad j+k \neq 3; \quad \beta = 2 \end{cases} \tag{9}$$

Constraints

Person Volume of Vehicles

The person volume of vehicles can be determined by the volume of vehicles and average number of passengers for private vehicles and buses, as shown in Eqs. (10) and (11)

$$Q_{iw}^{v} = n^{v} q_{iw}^{v}, \quad \forall\ i \in \mathcal{L}; \qquad w \in \{1,2,3\} \tag{10}$$

$$Q_{iw}^{v} = n^{b} q_{iw}^{v}, \quad \forall\ i \in \mathcal{L}; \qquad w \in \{4\} \tag{11}$$

Phase Plan of the Vehicles

The phase plan of dual ring is used in this study. The basic concept of the dual ring and the definition of a phase are illustrated in Fig. 4(a). It is extended from the following two aspects. First, the sequences of left-turning movement and through movement in each ring are allowed to be exchanged, which may affect the delay of the passengers. The first phases could be left-turn or through movement. As shown in Eqs. (12)–(23), the binary variables P_{EW} and

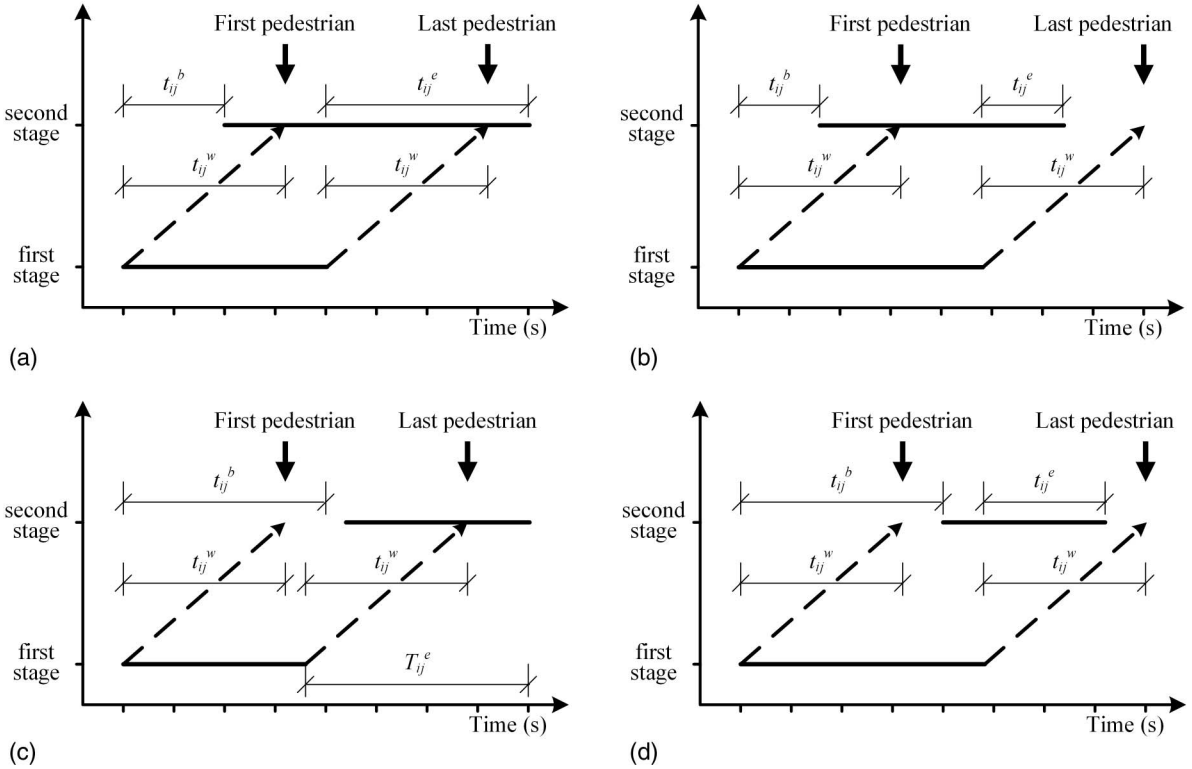

Fig. 3. Signal coordination of the two-stage crosswalk: (a) Type 1; (b) Type 2; (c) Type 3; (d) Type 4

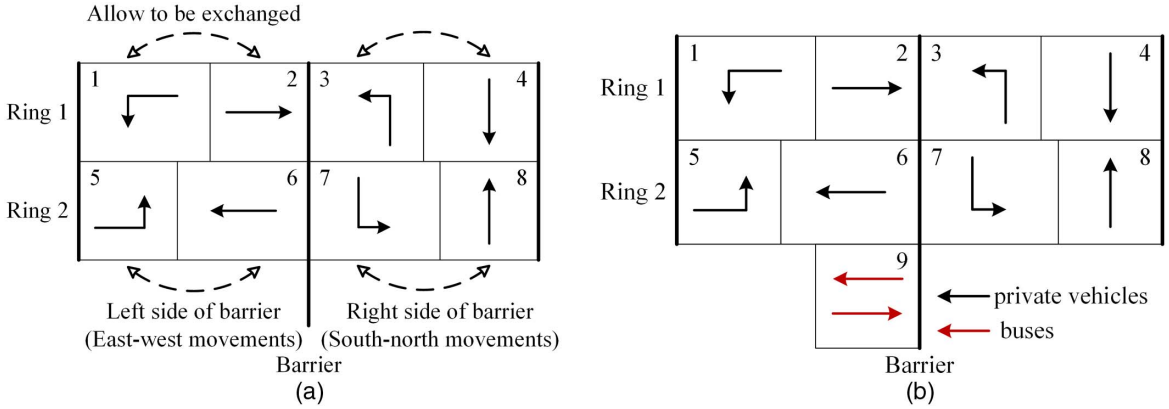

Fig. 4. Phase plan of the vehicles: (a) basic concept of dual ring; (b) phase for through movement of center transit lane

P_{SN} are used to indicate whether the left-turn movement leads the through movement (0 = yes and 1 = no) for east–west and south–north phases, respectively. If the left turn leads the through movement ($P_{EW} = 0$; $P_{SN} = 0$), Eqs. (12)–(17) will be active and Eqs. (18)–(23) will always be satisfied. On the contrary, if the through movement leads the left turn ($P_{EW} = 1$; $P_{SN} = 1$), Eqs. (18)–(23) will be active and Eqs. (12)–(17) will always be satisfied.

$$-MP_{EW} \le g_p^{vs} \le MP_{EW}; \quad \forall\ p \in \{1,5\} \tag{12}$$

$$g_p^{vs} + g_p^v + I - MP_{EW} \le g_{p+1}^{vs} \le g_p^{vs} + g_p^v + I + MP_{EW}; \quad \forall\ p \in \{1,5\} \tag{13}$$

$$g_p^{vs} + g_p^v + I - MP_{EW} \le g_{SN}^{vs} \le g_p^{vs} + g_p^v + I + MP_{EW}; \quad \forall\ p \in \{2,6\} \tag{14}$$

$$g_{SN}^{vs} - MP_{SN} \le g_p^{vs} \le g_{SN}^{vs} + MP_{SN}; \quad \forall\ p \in \{3,7\} \tag{15}$$

$$g_p^{vs} + g_p^v + I - MP_{SN} \le g_{p+1}^{vs} \le g_p^{vs} + g_p^v + I + MP_{SN}; \quad \forall\ p \in \{3,7\} \tag{16}$$

$$g_p^{vs} + g_p^v + I - MP_{SN} \le C \le g_p^{vs} + g_p^v + I + MP_{SN}; \quad \forall\ p \in \{4,8\} \tag{17}$$

$$-M(1 - P_{EW}) \le g_p^{vs} \le M(1 - P_{EW}); \quad \forall\ p \in \{2,6\} \tag{18}$$

$$g_p^{vs} + g_p^v + I - M(1 - P_{EW}) \le g_{p-1}^{vs} \le g_p^{vs} + g_p^v + I + M(1 - P_{EW}); \quad \forall\ p \in \{2,6\} \tag{19}$$

$$g_p^{vs} + g_p^v + I - M(1 - P_{EW}) \le g_{SN}^{vs} \le g_p^{vs} + g_p^v + I + M(1 - P_{EW}); \quad \forall\ p \in \{1,5\} \tag{20}$$

$$g_{SN}^{vs} - M(1 - P_{SN}) \le g_p^{vs} \le g_{SN}^{vs} + M(1 - P_{SN}); \quad \forall\ p \in \{4,8\} \tag{21}$$

$$g_p^{vs} + g_p^v + I - M(1 - P_{SN}) \le g_{p-1}^{vs} \le g_p^{vs} + g_p^v + I + M(1 - P_{SN}); \quad \forall\ p \in \{4,8\} \tag{22}$$

$$g_p^{vs} + g_p^v + I - M(1 - P_{SN}) \le C \le g_p^{vs} + g_p^v + I + M(1 - P_{SN}); \quad \forall\ p \in \{3,7\} \tag{23}$$

Second, the through movement of the center transit lane cannot discharge simultaneously with the left-turn lane in the same leg. Therefore, the phase for the through movement of the center transit lane is added as illustrated in Fig. 4(b). Under the case that the left-turn movement leads through, the start of green for the through movement of the center transit lane should be equal to the larger of the starts for green of the eastbound and westbound through movement, and the end of green should be equal to the end of the east–west movement, as shown in Eqs. (24)–(26). Under the case that through movement leads left-turn movement, the start of green of the through movement of the center transit lane should be equal to the start of east–west movement, and the duration of green should be equal to the smaller of the durations of green for the eastbound and westbound through movement, as shown in the following Eqs. (27)–(29):

$$g_p^{vs} \ge g_2^{vs} - MP_{EW}; \quad \forall\ p \in \{9\} \tag{24}$$

$$g_p^{vs} \ge g_6^{vs} - MP_{EW}; \quad \forall\ p \in \{9\} \tag{25}$$

$$g_p^{vs} + g_p^v + I - MP_{EW} \le g_{SN}^{vs} \le g_p^{vs} + g_p^v + I + MP_{EW}; \quad \forall\ p \in \{9\} \tag{26}$$

$$-M(1 - P_{EW}) \le g_p^{vs} \le M(1 - P_{EW}); \quad \forall\ p \in \{9\} \tag{27}$$

$$g_p^v \le g_2^v + M(1 - P_{EW}); \quad \forall\ p \in \{9\} \tag{28}$$

$$g_p^v \le g_6^v + M(1 - P_{EW}); \quad \forall\ p \in \{9\} \tag{29}$$

Phase Plan of the Pedestrians

The signal for pedestrians should operate in harmony with the signal for vehicles, as illustrated in Fig. 5. If the crosswalks on Legs 2 and 4 are one-stage crosswalks, pedestrians on Legs 2 and 4 can cross the intersection during Phases 2 and 6, respectively, as shown in Eqs. (30)–(33). For the two-stage crosswalk, each segment of the crosswalk could be controlled separately. According to Fig. 5, the start and duration of green for each segment of the crosswalk can be calculated as in Eqs. (34)–(49). Crosswalks on Legs 1 and 3 are always two-stage crosswalks to allow the existence of the center transit lane stops

$$g_{2j0}^{ps} = g_2^{vs}; \quad \forall\ j \in \mathcal{J} \tag{30}$$

$$g_{2j0}^{p} + T_{2j0}^{w} = g_2^{v}; \quad \forall\ j \in \mathcal{J} \tag{31}$$

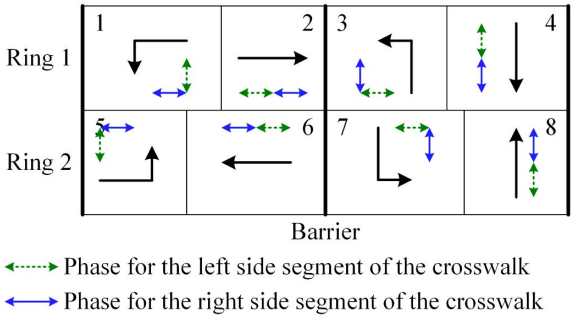

Fig. 5. Phase plan of the pedestrians

$$g_{4j0}^{ps} = g_6^{vs}; \quad \forall\ j \in \mathcal{J} \tag{32}$$

$$g_{4j0}^{p} + T_{4j0}^{w} = g_6^{v}; \quad \forall\ j \in \mathcal{J} \tag{33}$$

$$g_{1j1}^{ps} = g_8^{vs}; \quad \forall\ j \in \mathcal{J} \tag{34}$$

$$g_{1j1}^{p} + T_{1j1}^{w} = g_8^{v} + g_1^{v} + I; \quad \forall\ j \in \mathcal{J} \tag{35}$$

$$g_{1j2}^{ps} = g_7^{vs}; \quad \forall\ j \in \mathcal{J} \tag{36}$$

$$g_{1j2}^{p} + T_{1j2}^{w} = g_7^{v} + g_8^{v} + I; \quad \forall\ j \in \mathcal{J} \tag{37}$$

$$g_{2j1}^{ps} = g_2^{vs}; \quad \forall\ j \in \mathcal{J} \tag{38}$$

$$g_{2j1}^{p} + T_{2j1}^{w} = g_2^{v} + g_3^{v} + I; \quad \forall\ j \in \mathcal{J} \tag{39}$$

$$g_{2j2}^{ps} = g_1^{vs}; \quad \forall\ j \in \mathcal{J} \tag{40}$$

$$g_{2j2}^{p} + T_{2j2}^{w} = g_1^{v} + g_2^{v} + I; \quad \forall\ j \in \mathcal{J} \tag{41}$$

$$g_{3j1}^{ps} = g_4^{vs}; \quad \forall\ j \in \mathcal{J} \tag{42}$$

$$g_{3j1}^{p} + T_{3j1}^{w} = g_4^{v} + g_5^{v} + I; \quad \forall\ j \in \mathcal{J} \tag{43}$$

$$g_{3j2}^{ps} = g_3^{vs}; \quad \forall\ j \in \mathcal{J} \tag{44}$$

$$g_{3j2}^{p} + T_{3j2}^{w} = g_3^{v} + g_4^{v} + I; \quad \forall\ j \in \mathcal{J} \tag{45}$$

$$g_{4j1}^{ps} = g_6^{vs}; \quad \forall\ j \in \mathcal{J} \tag{46}$$

$$g_{4j1}^{p} + T_{4j1}^{w} = g_6^{v} + g_7^{v} + I; \quad \forall\ j \in \mathcal{J} \tag{47}$$

$$g_{4j2}^{ps} = g_5^{vs}; \quad \forall\ j \in \mathcal{J} \tag{48}$$

$$g_{4j2}^{p} + T_{4j2}^{w} = g_5^{v} + g_6^{v} + I; \quad \forall\ j \in \mathcal{J} \tag{49}$$

Limitation of the Signal Timing Parameters

Eq. (50) limits the cycle length to be within the reasonable range between C_{min} and C_{max}

$$C_{min} \le C \le C_{max} \tag{50}$$

In order to avoid sudden stop-and-go motions, the minimum green time for the vehicles should be set as shown in Eq. (51)

$$g_p^v \geq g_{\min}; \quad \forall\ p \in \mathcal{P} \tag{51}$$

The maximum waiting time for the pedestrians should be limited to within the length that the pedestrians can tolerate, as shown in Eq. (52)

$$C - g_{ijk}^p \leq R_{\max}, \quad \forall\ i \in \mathcal{L}; \qquad j \in \mathcal{J}; \qquad p \in \mathcal{P} \tag{52}$$

Moreover, in the pedestrian delay calculation model [Eq. (7)], there are two key parameters: (1) time length between the beginnings of the first-stage and second-stage walk intervals (t_{ij}^b); and (2) time length between the ends of the first-stage and second-stage walk intervals (t_{ij}^e). They can be determined by Eqs. (53) and (54), respectively

$$t_{ij}^b = g_{ijk}^{ps} - g_{ijk'}^{ps}; \quad \forall\ i \in L; \qquad j \in \mathcal{J}; \qquad k = j; \qquad k' \in \mathcal{K}; \qquad k \neq k' \tag{53}$$

$$t_{ij}^e = g_{ijk}^{ps} + g_{ijk}^p - g_{ijk'}^{ps} - g_{ijk'}^p; \quad \forall\ i \in L; \qquad j \in \mathcal{J}; \qquad k = j; \qquad k' \in \mathcal{K}; \qquad k \neq k' \tag{54}$$

In the passenger delay calculation model [Eq. (9)], there are two key parameters: (1) time length between the beginnings of the walk interval of the crosswalk and green time of the center transit lane (δ_{ijk}^e); and (2) time length between the beginning of the walk interval of the crosswalk and end of the green time of the center transit lane (δ_{ijk}^e). They can be determined by Eqs. (55) and (56), respectively

$$\delta_{ijk}^b = g_{ijk}^{ps} - g_p^{vs}; \quad \forall\ i \in \{1,3\}; \qquad j \in \mathcal{J}; \qquad k \in \mathcal{K}; \qquad p \in \{9\} \tag{55}$$

$$\delta_{ijk}^e = g_{ijk}^{ps} - g_p^{vs} - g_p^v; \quad \forall\ i \in \{1,3\}; \qquad j \in \mathcal{J}; \qquad k \in \mathcal{K}; \qquad p \in \{9\} \tag{56}$$

Limitation of the Central Refuge Island Waiting Area

The people waiting on the central refuge island includes two groups: (1) crossing pedestrians, and (2) alighting passengers. The worst condition occurs at the end of the red signal of the central refuge island. According to Figs. 2(c–f), the maximum number of crossing pedestrians waiting on the central refuge island of each crossing direction can be calculated by Eq. (57). The number of crossing pedestrians waiting on the central refuge island at the end of the red equals the sum of pedestrians of the two crossing directions, as shown in Eq. (58)

$$N_{ij}^{pe} = \begin{cases} 0, & \forall\ i \in \mathcal{L}; \quad j \in \mathcal{J}; \quad T_{ij}^b < T_{ij}^w; \quad T_{ij}^e > T_{ij}^w \\ (T_{ij}^w - T_{ij}^e)\dfrac{Q_{ij}^{pe}}{3,600}; & \forall\ i \in \mathcal{L}; \quad j \in \mathcal{J}; \quad T_{ij}^b < T_{ij}^w; \quad T_{ij}^e < T_{ij}^w \\ (C - g_{ij1}^p + T_{ij}^b - T_{ij}^w)\dfrac{Q_{ij}^{pe}}{3,600}; & \forall\ i \in \mathcal{L}; \quad j \in \mathcal{J}; \quad T_{ij}^b > T_{ij}^w; \quad T_{ij}^e > T_{ij}^w \\ (C - g_{ij1}^p + T_{ij}^b - T_{ij}^e)\dfrac{Q_{ij}^{pe}}{3,600}; & \forall\ i \in \mathcal{L}; \quad j \in \mathcal{J}; \quad T_{ij}^b > T_{ij}^w; \quad T_{ij}^e < T_{ij}^w \end{cases} \tag{57}$$

$$N_i^{pe} = \sum_{j \in \mathcal{J}} N_{ij}^{pe}; \quad \forall\ i \in L \tag{58}$$

The maximum number of passengers waiting on the central refuge island depends on the location of the bus stops and the signal timing. If the bus stop is located at the near side of the intersection [Fig. 2(g)], the passengers arrive randomly. Only passengers who arrive during the red signal of the crosswalk must wait at the central refuge island. If the bus stop is located at the far side of the intersection [Fig. 2(h)], the passengers arrive during the green time of the center transit lane. Therefore, all the passengers have to wait at the central refuge island. The number of passengers waiting on the central refuge island at the end of the red can be calculated by Eq. (59)

$$N_i^{pa} = \begin{cases} \sum_{j \in \mathcal{J}} \sum_{k=1,2} (C - g_{ijk}^p)\dfrac{Q_{ijk}^{pa}}{3,600}; & \forall\ i \in \{1,3\}; \quad j + k \neq 3; \quad \beta = 1 \\ \sum_{j \in \mathcal{J}} \sum_{k=1,2} \dfrac{C Q_{ijk}^{pa}}{3,600}; & \forall\ i \in \{1,3\}; \quad j + k \neq 3; \quad \beta = 2 \end{cases} \tag{59}$$

Therefore, the total number of people waiting on the central island of both directions can be calculated by Eq. (60), which should be below the maximum acceptable number of people for safety purposes

$$\frac{A_i}{A_{p\min}} \geq N_i^p = N_i^{pe} + N_i^{pa}, \quad \forall\ i \in \mathcal{L} \tag{60}$$

Solution Algorithm

With the objective function of Eqs. (1) and (2) and constraints of Eqs. (3)–(60), the proposed optimization model is a two-objective (bicriteria) nonlinear programming model including competing objectives. It could be treated by trade-off analysis using the notion of a Pareto-optimal solution (Nakayama et al. 2009). Each Pareto point is a solution of the multiobjective optimization problem.

All Pareto solutions comprise a Pareto frontier (Bai et al. 2015). A designer selects the ultimate solution from among the Pareto set based on additional requirements, which may be subjective. Therefore, the proposed optimization model can be reduced to the maximization of an aggregate objective function with a linear (weighted) combination of the objective functions, as shown in Eq. (62). This is the simplest and often used classical method to treat the multiobjective problem (Erfani and Utyuzhnikov 2011). Then, the Pareto frontiers of the proposed model could be drawn by iterating all possible combinations of weights that correspond to the decision maker's expectations (Messac and Messac 2000). For each combination of weights, the optimization turns into single-objective mixed-integer nonlinear programming. A GA-based heuristic method was used for yielding optimal signal solutions to the model. GA-based heuristics have been successfully demonstrated in previous works for similar optimization problems (Ma et al. 2011, 2015; Zhao et al. 2016)

$$\max \alpha^v D^v + (1 - \alpha^v) D^p \tag{61}$$

Performance Analysis

The proposed model was first applied to a case study to assess its effectiveness. The impacts of the various traffic patterns and geometric configurations on vehicular and pedestrian operations were further investigated through sensitivity analyses.

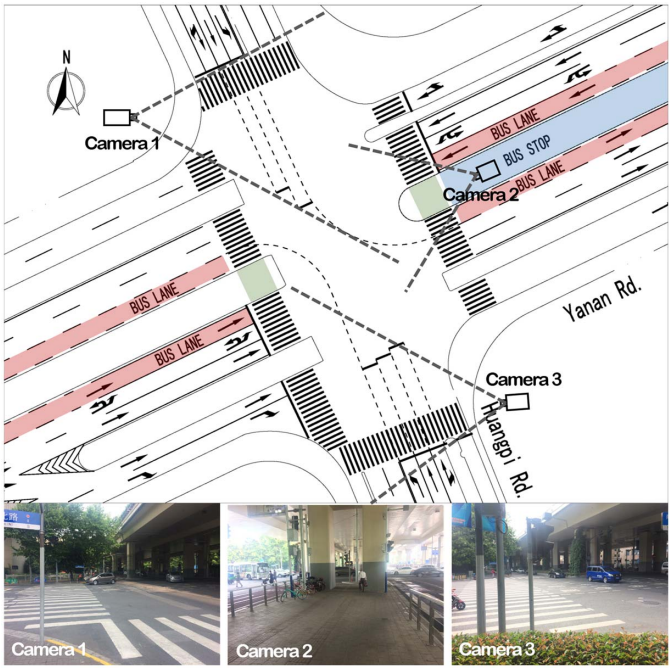

Fig. 6. Layout of the case study intersection and field survey

Case Study

An intersection at Yanan Road and Huangpi Road in Shanghai, China was used to evaluate the performance of the proposed model. The layout of the study intersection is illustrated in Fig. 6. There is a center transit lane on Yanan Road. The bus stops for the two directions are located on the east leg of the intersection. The operational condition was obtained by a field survey using video cameras, as shown in Fig. 6. The traffic demand is summarized in Table 1. The original signal timing scheme is illustrated in Fig. 7. The crossing time of the half length of east and west crosswalks are 20 and 23 s, respectively, and that of the entire length of the south and north crosswalks are 26 and 20 s, respectively, under the assumption that the crossing speed is 1 m/s (TRB 2010). The average number of passengers for buses and for private vehicles are 40 and 2 persons/vehicle. The minimum acceptable average pedestrian space is 0.5 m^2/person according to the level of Service D for pedestrian queuing areas (TRB 2010). The saturation flow rate of a lane is 1,800 vehicles/h (TRB 2010). The minimum and maximum cycle lengths are set to be 120 and 180 s, respectively, for the condensation of the heavy traffic demand of the intersection. The clearance time between mutually incompatible traffic movements is 5 s according to the geometric layout. The minimum green time is 10 s (TRB 2010).

The proposed model is implemented, and the original design is not on the optimal frontier, as illustrated in Fig. 8. Three optimized signal timing schemes are used for further comparison.

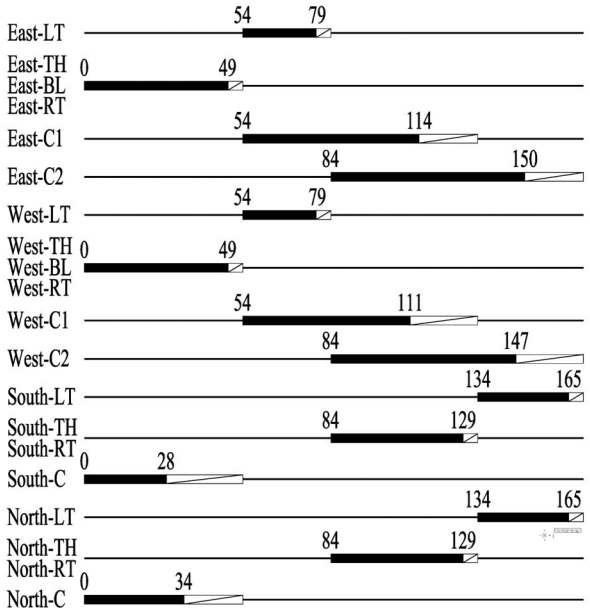

Fig. 7. Original signal timing

Table 1. Traffic Demand

Leg	Movement						
	Left turn	Through movement	Bus lane	Right turn	Left-side segment of the two-stage crosswalk[a]	Right-side segment of the two-stage crosswalk[a]	One-stage crosswalk[a]
East	192	772	20	184	410, 390, 155, 142	410, 390, 150, 160	—
West	218	792	20	243	420, 430, 0, 0	420, 430, 0, 0	—
South	289	520	—	222	—	—	350, 360, 0, 0
North	283	506	—	207	—	—	450, 430, 0, 0

[a]The four numbers indicate the clockwise-direction crossing pedestrians, anticlockwise-direction crossing pedestrians, boarding passengers, and alighting passengers, respectively.

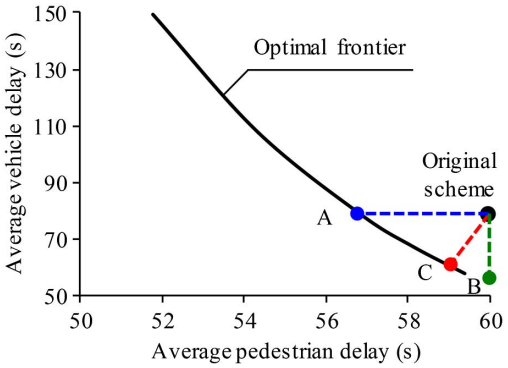

Fig. 8. Optimal frontier of the case study

Scheme 1 improves the performance of the pedestrians while retaining the performance of the vehicles (Point A in Fig. 8). Scheme 2 improves the performance of the vehicles while retaining the performance of the pedestrians (Point B in Fig. 8). Scheme 3 uses the person volume as the weightage ($\alpha^v = 0.73$) (Point C in Fig. 8). The optimized signal timing schemes are listed in Fig. 9. The microscopic simulation package *VISSIM* was used as the unbiased evaluator to assess the performance of the model. To overcome the stochastic nature of a microscopic simulation system, an average of 10 simulation runs were used. The delays of vehicles and pedestrians were used for evaluation. The results are provided in Table 2.

It can be observed that the Scheme 1 can reduce the pedestrian delay by 5.3% while maintaining the vehicle delay of the original

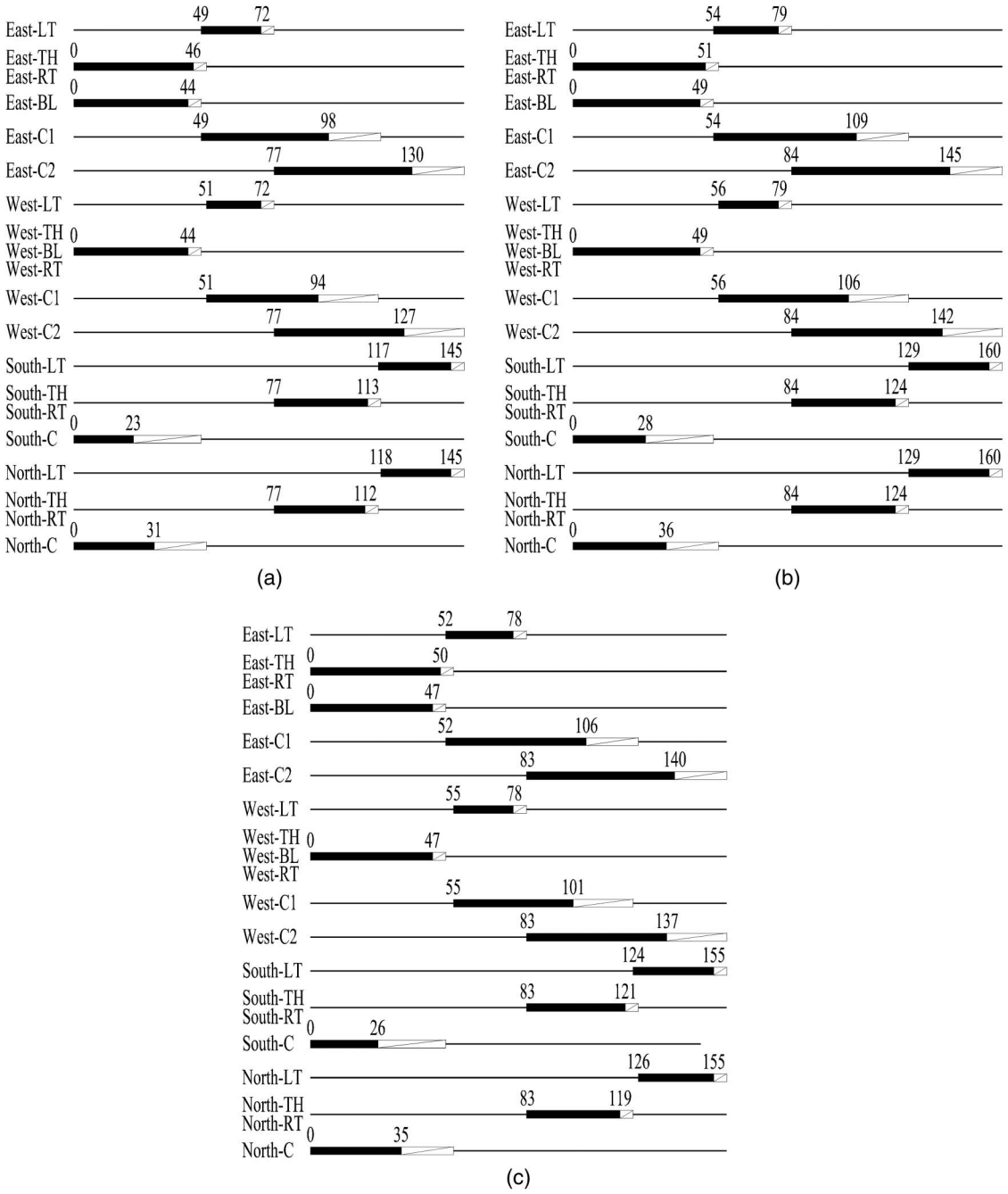

Fig. 9. Optimized signal timing schemes: (a) Scheme 1; (b) Scheme 2; (c) Scheme 3

J. Transp. Eng., Part A: Systems, 2018, 144(6): 04018023

Table 2. Performance Evaluation

Traveler	Original delay (s)	Scheme 1		Scheme 2		Scheme 3	
		Delay (s)	Improvement (%)	Delay (s)	Improvement (%)	Delay (s)	Improvement (%)
Private vehicles	85.0	85.5	0.6	61.2	−28.0	60.7	−28.6
Buses	41.6	41.1	−1.2	42.5	2.2	42.1	1.2
Crossing pedestrians	64.4	60.9	−5.4	65.1	1.1	63.7	−1.1
Passengers	36.5	35.1	−3.8	37.0	1.3	36.3	−0.4
Average of vehicles	78.4	78.1	0.4	58.3	−25.5	57.9	−26.1
Average of pedestrians	60.0	56.8	−5.3	60.7	1.1	59.4	−1.0
Per capita	73.4	72.8	−0.8	59.0	−19.7	58.3	−20.6

Table 3. Basic Input Parameters for Sensitivity Analyses

Parameter	Value
Traffic volume of private vehicles on a leg	700 vehicles/h
Traffic volume of buses on a leg	50 vehicles/h
Left-turn ratio	50%
Pedestrian volume on a crosswalk	2,000 persons/h
Passenger boarding and alighting volumes	1,000 persons/h
Average number of passengers for buses	40 persons/vehicle
Average number of passengers for private vehicles	2 persons/vehicle
Saturation flow rate of vehicles for each movement	1,800 vehicles/h
Location of the center transit lane stop	Near side
One-stage or two-stage crosswalk	Two-stage crosswalk at each leg
Minimum acceptable average pedestrian space	0.5 m^2/person
Minimum and maximum cycle length	60 and 180 s
Crossing time of the crosswalk	10 s
Minimum green time	10 s

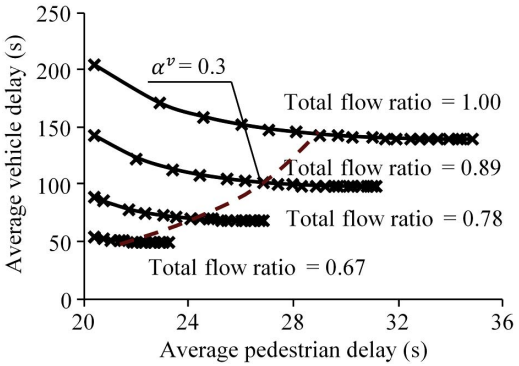

Fig. 10. Optimal frontier under different flow ratio cases

scheme. Scheme 2 can reduce the vehicle delay by 25.5% while maintaining the pedestrian delay of the original scheme. Scheme 3 can reduce the vehicle delay and pedestrian delay by 26.1 and 1.0%, respectively. Overall, the three schemes can reduce the per capita delays by 0.8, 19.7, and 20.6%, respectively, using the original scheme as the benchmark, which demonstrates the effectiveness of the proposed model.

Sensitivity Analyses

A four-leg intersection with center transit lane stops is considered. The basic input parameters are given in Table 3. These parameters will be changed as needed when analyzing the sensitivity of the parameter.

Impact of Flow Ratio

Because the delay of a vehicle is closely related to the flow ratio, four levels of traffic volume of private vehicles were set (600, 700, 800, and 900 vehicles/h) to analyze the impact of vehicular flow ratio on the intersection performance. The optimal frontiers of the three traffic volume cases are shown in Fig. 10. The weight of the vehicle (α^v) increases from 0 to 1 when the lines in Fig. 10 go from left to right. In general, with an increase in vehicular flow ratio, delays to both vehicle and pedestrian also increase. Moreover, with the increase in weight of the vehicle (from left to right of the optimal frontiers), the average vehicle delay decreases while the average pedestrian delay increases. This indicates the incompatibility between the performance of vehicles and pedestrians. However, the average vehicle delay decreases rapidly with the increase in weight of the vehicle and reaches a low value platform when the weight of the vehicle is larger than 0.3.

Impact of Cycle Length

For signal timing, cycle length is a key factor for balancing the trade-off between vehicles and pedestrians. From the pedestrians' (including crossing pedestrian and bus passenger) point of view, for cycle length, the shorter the better, whereas from the vehicles' (including the private vehicles and buses) point of view, there exists an optimal value of cycle length, as illustrated in Fig. 11(a). Therefore, with the increase in weight factor for vehicles from 0 (performance of vehicles is neglected) to 1 (performance of pedestrians is neglected), the optimal cycle length also increases, as illustrated in Fig. 11(b). This indicates that from the point of view of pedestrians, the current vehicle-based signal timing always leads to long cycle length for pedestrians.

Fig. 11(c) further analyzes the number of people waiting at the central refuge island under different cycle length cases. There is significant incense in the number of people waiting at the central refuge island with an increase in cycle length. If there are no center transit lane stops, the number of pedestrians waiting at the central refuge island is acceptable (fewer than 20 persons). However, when adding alighting passengers, there are too many people on the central refuge island, which may cause safety problems. On average, an 80% shorter cycle length is recommended.

Impact of Bus Stop Location

Although the center transit lane can improve the performance of buses, all alighting passengers have to get off the buses and cross the street from the center transit lane stops. The bus stops for the center transit lane can be set at the near side or far side of the approach. As shown in Fig. 12(a), the location of the bus stop does not affect the delay of the boarding passengers because their delay is owing to the fact that they arrive randomly, no matter where

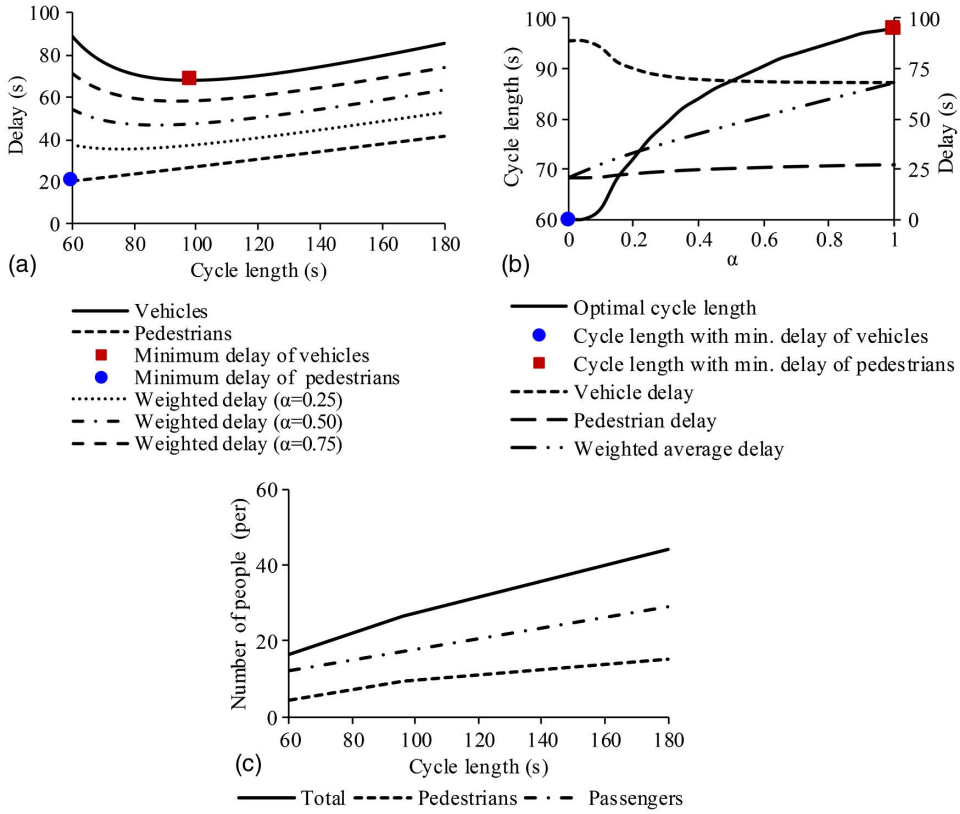

Fig. 11. Impact of cycle length analysis: (a) change tendency of delay with the cycle length; (b) optimal cycle length under different weight factors; (c) change tendency of people waiting at the central island with the cycle length

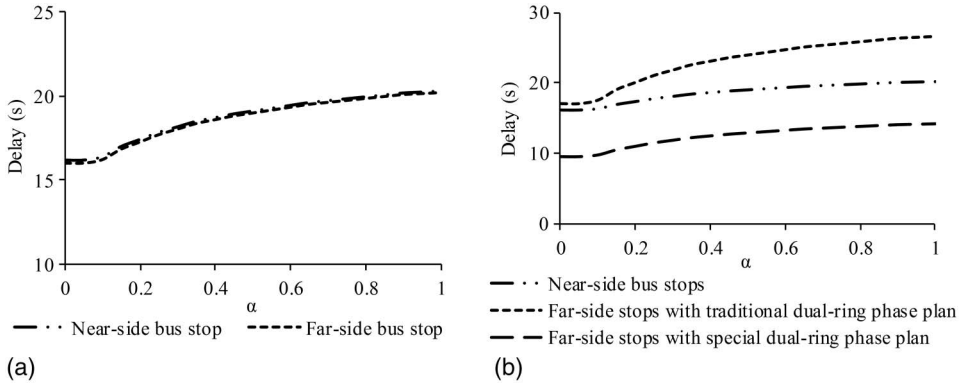

Fig. 12. Impact of location of bus stop on passenger delay: (a) boarding passengers; (b) alighting passengers

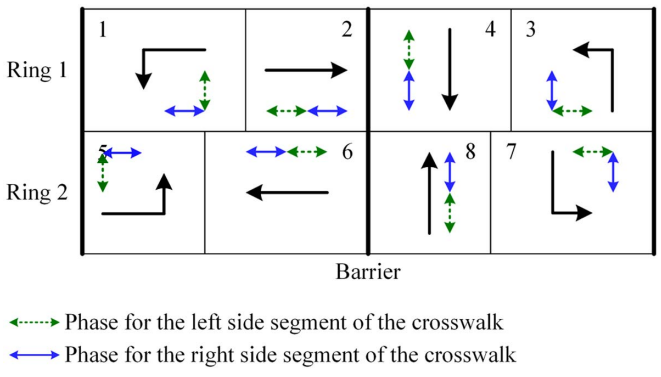

Fig. 13. Special dual-ring phase plan for passengers

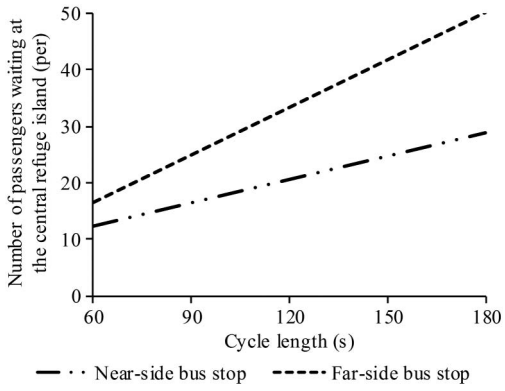

Fig. 14. Number of waiting passengers for the two types of bus stop location

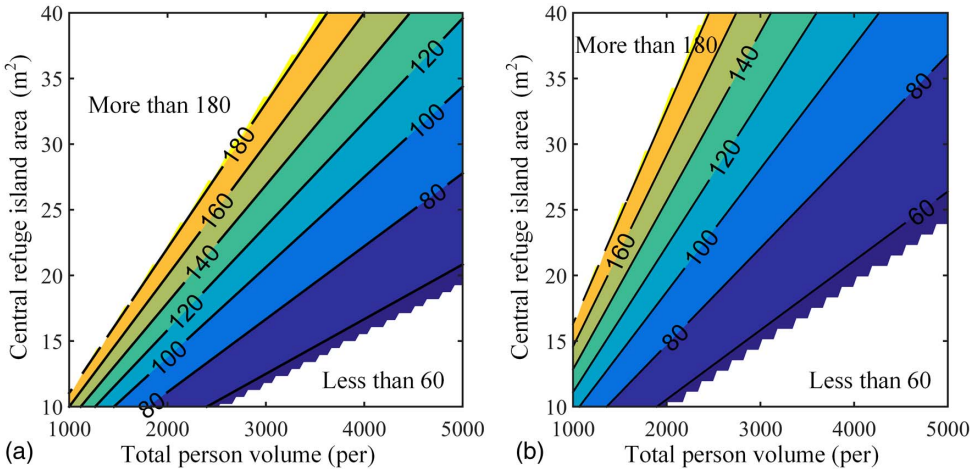

Fig. 15. Limitation of the cycle length for the two types of bus stop location: (a) near-side bus stop; (b) far-side bus stop

the bus stop is located. However, the delay of alighting passengers is different for different bus stop location cases. If the bus stop is located at the near side of the intersection, passengers arrive randomly. If the bus stop is located at the far side of the intersection, passengers arrive during the green time of the center transit lane. Then, according to the traditional dual-ring phase plan (Fig. 5), passengers can use the right side of the crosswalks on Legs 1 and 3 in the following phase, whereas passengers who want to use the left side of the crosswalks have to wait until the phase after the next starts. Therefore, when the traditional dual-ring phase plan is used, far-side bus stops lead to longer delay (11% increase on average) of passengers compared with the near-side bus stops. However, if the phase sequence of the left-turn movement and through movement is changed (Fig. 13), all the alighting passengers can depart in the following phase. Then, the delay can be greatly reduced (45% reduction on average), as shown in Fig. 12(b).

Besides the delay of passengers, the location of the bus stop also affects the number of people waiting on the central refuge island. For the near-side bus stop condition, when the buses arrive during the green time of the crosswalk, passengers can cross the street after getting off the buses; otherwise, passengers have to wait at the central refuge island. The setting of the bus stops leads to twice as many people waiting at the central refuge island in comparison with the condition without the bus stops. However, if the bus stop is located at the far side of the intersection, all alighting passengers have to wait at the central refuge island because the buses always arrive at the bus stop during the red time of the crosswalk. The comparison of the number of passengers waiting at the central refuge island under the two types of bus stop location is shown in Fig. 14. On average, 60% more passengers are waiting at the central refuge island under the far-side bus stop condition. Therefore, a bigger waiting area is needed for the central refuge island. Moreover, a shorter cycle length should be used to reduce the number of passengers waiting at the central refuge. The limitation of the cycle length under different combinations of passenger volumes and central refuge island area is shown in Fig. 15. Another way to relieve this problem is to use the special dual-ring phase plan in Fig. 13, which can reduce the duration of the worst condition.

Conclusions

A signal timing model for intersections with a center transit lane and bus stops was presented in this paper. Four kinds of traffic travelers were considered, namely, private vehicles, buses, crossing pedestrians, and passengers. To balance the trade-off between their operations, an optimization model was formulated as a two-objective programming problem using the weighted average person delay as the objective. The Pareto frontier of solutions obtained with the proposed model was drawn by iterating all possible combinations of weights. The performance of the proposed model was evaluated using a case study and extensive numerical analyses. The following conclusions can be drawn from the results:

- The proposed model could provide improved decisions for the signal timing to balance the trade-off between vehicles and pedestrians. The average vehicle delay decreases rapidly with the increase in weight of the vehicle and reaches a low value platform when the weight of the vehicle is larger than 0.3;
- For the signal timing, cycle length is a key factor for balancing the trade-off between vehicles and pedestrians. On average, an 80% shorter cycle length in comparison with the vehicle-based signal timing is recommended in consideration of both the overall performance and number of people waiting on the central refuge island. Moreover, the phase plan is a key factor for the smooth departure of bus passengers. A special dual-ring phase plan in Fig. 13 is recommended when the bus stop is located at the far side of the intersection to ensure all the alighting passengers can depart at the following phase; and
- For the geometric design, the location of the bus stops and central refuge island area are two key factors for the good operation of the intersections. On average, there are 11% more delays and 60% more passengers waiting at the central refuge island under the far-side bus stop condition. Moreover, a larger waiting area is needed for central refuge island for intersections with center transit lane stops.

This paper used a deterministic analysis method. Therefore, future work will introduce a stochastic analysis to maintain stable performance under fluctuating traffic demand conditions. Moreover, transit-signal priority and actuated control for pedestrians could be added to further improve the overall performance of the intersections. In practice, right turns on red should not be allowed, and pedestrians must not violate the traffic signal indications. The weight factors of vehicles and pedestrians can be changed according to traffic-flow variations in different time periods (e.g., peak and off-peak hours) or day categories (e.g., weekdays, weekends, and holidays).

Acknowledgments

The research is supported by the National Natural Science Foundation of China under Grant No. 51608324.

Notation

The following symbols are used in this paper:

A_i = central island space on leg i (m^2);
$A_{p\min}$ = minimum acceptable average pedestrian space (m^2/person);
C = cycle length (s);
$C_{\min}, C_{\max}$ = minimum and maximum cycle length (s);
D^p = weighted average delay of pedestrians (s);
D^v = weighted average delay of vehicles (s);
d_{ij}^{pe} = delay of crossing pedestrians for movement j on leg i (s);
d_{iw}^{v} = delay of vehicles for movement w on leg i (s);
d_{ij}^{pe1} = delay of crossing pedestrians for the one-stage crosswalk for movement j on leg i (s);
d_{ij}^{pe2} = delay of crossing pedestrians for the two-stage crosswalk for movement j on leg i (s);
d_{ijk}^{pa} = delay of passengers for movement j on leg i segment k (s);
g_{ijk}^{p} = green time (also called walk time) of the crosswalk for movement j on leg i at segment k (s);
g_{ijk}^{ps} = start of green of the crosswalk for movement j on leg i at segment k (s);
g_{iw}^{v} = green time of vehicles for movement w on leg i (s);
$g_{\min}$ = minimum green time (s);
g_p^v = green time of vehicles for phase p (s);
g_p^{vs} = start of green of vehicles for phase p (s);
g_{SN}^{vs} = start of green of vehicles for south–north phases (s);
I = clearance time for a pair of conflicting traffic movements (s), which includes the amber period and all-red period;
$i \in \mathcal{L}$ = index of legs; $i = 1$ for east leg, $i = 2$ for south leg, $i = 3$ for west leg, and $i = 4$ for north leg, as illustrated in Fig. 1;
$\mathcal{J}$ = set of pedestrian movements;
$j \in \mathcal{J}$ = index of pedestrian movements; $j = 1$ for the clockwise direction, and $j = 2$ for the anticlockwise direction, as illustrated in Fig. 1;
$k \in \mathcal{K}$ = index of segment of the crosswalk; $k = 0$ for the one-stage crosswalk, $k = 1$ for the left side of the leg of the two-stage crosswalk, and $k = 2$ for the right side of the leg of the two-stage crosswalk, as illustrated in Fig. 1;
$\mathcal{L}$ = set of legs;
M = arbitrarily large positive constant number, which is set to be 10^9 in this model;
N_i^p = total number of people waiting on the central island on leg i;
N_i^{pa} = number of passengers waiting on the central island on leg i;
N_i^{pe} = number of pedestrians waiting on the central island on leg i;
n^b = average number of passengers for buses (person/vehicle);
n^v = average number of passengers for private vehicles (person/vehicle);
$\mathcal{P}$ = set of signal phases;
$P_{\mathrm{EW}}, P_{\mathrm{SN}}$ = binary variables indicating whether the left turn leads through (0 = yes; 1 = no) for east–west phases and south–north phases, respectively;
$p \in \mathcal{P}$ = index of signal phase; $p = 1$ for the westbound left turn, $p = 2$ for the eastbound through, $p = 3$ for the northbound left turn, $p = 4$ for the southbound through, $p = 5$ for the eastbound left turn, $p = 6$ for the westbound through, $p = 7$ for the southbound left turn, $p = 8$ for the northbound through, and $p = 9$ for the through of center transit lane, as illustrated in Fig. 4;
Q_{ij}^{pe} = person volume of crossing pedestrians for movement j on leg i (persons/h);
Q_{ijk}^{pa} = person volume of passengers for movement j on leg i segment k (persons/h);
Q_{iw}^{v} = person volume of vehicles for movement w on leg i (persons/h);
q_{iw}^{v} = volume of vehicles for movement w on leg i (vehicles/h);
s_{iw}^{v} = saturation flow rate of vehicles for movement w on leg i (vehicles/h);
$\mathcal{T}$ = set of vehicular movements;
T = duration of analysis period, which is set to be 1 in this study;
T_{ijk}^{w} = crossing time (also called the FDW time) of the crosswalk for movement j on leg i at segment k (s);
t_{ij}^{b} = time length between beginnings of the first-stage and second-stage walk intervals (green time of pedestrians) for movement j on leg i (s);
t_{ij}^{e} = time length between nds of the first-stage and second-stage walk intervals (green time of pedestrians) for movement j on leg i (s);
$w \in \mathcal{T}$ = index of vehicular movements; $w = 1$ for left-turn, $w = 2$ for through movement, $w = 3$ for right-turn, and $w = 4$ for through movement of center transit lane, as illustrated in Fig. 1;
α^v = weight factors for vehicles;
β = location of the center transit lane stop; $\beta = 1$ for near side, and $\beta = 2$ for far side;
δ_{ijk}^{b} = time length between the beginnings of the walk interval of movement j on leg i segment k and green time for the center transit lane (s);
δ_{ijk}^{e} = time length between the beginning of the walk interval of movement j on leg i segment k and the end of green time for the center transit lane (s);
$\mathcal{K}$ = set of segments of the crosswalk; and
Ψ = set of traffic movement and signal phase pair; $(iw, p) \in \Psi$ for the permission of movement w from leg i at phase p.

References

Abdelghany, K. F., Mahmassani, H. S., and Abdelghany, A. F. (2007). "A modeling framework for bus rapid transit operations evaluation and service planning." *Transp. Plann. Technol.*, 30(6), 571–591.

Allsop, R. E. (1971). "SIGSET: A computer program for calculating traffic signal settings." *Traffic Eng. Control*, 13(2), 58–60.

Bai, Q., Ahmed, A., Li, Z., and Labi, S. (2015). "A hybrid Pareto frontier generation method for trade-off analysis in transportation asset management." *Comput.-Aided Civ. Infrastruct. Eng.*, 30(3), 163–180.

Balke, K. N., Dudek, C. L., and Thomas Urbanik, I. I. (2000). "Development and evaluation of intelligent bus priority concept." *Trans. Res. Rec.*, 1727, 12–19.

Bechtel, A., Macleod, K., and Ragland, D. (2004). "Pedestrian scramble signal in Chinatown neighborhood of Oakland, California: An evaluation." *Trans. Res. Rec.*, 1878, 19–26.

Cascetta, E., Gallo, M., and Montella, B. (2006). "Models and algorithms for the optimization of signal settings on urban networks with stochastic assignment models." *Ann. Oper. Res.*, 144(1), 301–328.

Chen, X. M., Yu, L., Zhang, Y. S., and Guo, J. F. (2009). "Analyzing urban bus service reliability at the stop, route, and network levels." *Transp. Res. Part A: Policy Pract.*, 43(8), 722–734.

Chilukuri, V., and Virkler, M. R. (2005). "Validation of HCM pedestrian delay model for interrupted facilities." *J. Transp. Eng.*, 10.1061/(ASCE)0733-947X(2005)131:12(939), 939–945.

Diakaki, C., Papageorgiou, M., Dinopoulou, V., Papamichail, I., and Garyfalia, M. (2015). "State-of-the-art and -practice review of public transport priority strategies." *IET Intell. Transp. Syst.*, 9(4), 391–406.

Duerr, P. A. (2000). "Dynamic right-of-way for transit vehicles: Integrated modeling approach for optimizing signal control on mixed traffic arterials." *Transp. Res. Rec.*, 1731, 31–39.

El Esawey, M., and Sayed, T. (2013). "Analysis of unconventional arterial intersection designs (UAIDs): State-of-the-art methodologies and future research directions." *Transportmetrica A: Transp. Sci.*, 9(10), 860–895.

Erfani, T., and Utyuzhnikov, S. V. (2011). "Directed search domain: A method for even generation of the Pareto frontier in multiobjective optimization." *Eng. Optim.*, 43(5), 467–484.

Fitzpatrick, K., and Turner, S. (2007). "Improving pedestrian safety at unsignalized intersections." *ITE J. Inst. Transp. Eng.*, 77(5), 34–41.

Furth, P. G., and Muller, T. H. J. (2000). "Conditional bus priority at signalized intersections: Better service with less traffic disruption." *Transp. Res. Rec.*, 1731, 23–30.

Goh, P. K., and Lam, W. H. K. (2004). "Pedestrian flows and walking speed: A problem at signalized crosswalks." *ITE J.*, 74(1), 28–33.

Griffiths, J. D., Hunt, J. G., and Marlow, M. (1985). "Delays at pedestrian crossings. IV: Mathematical models." *Traffic Eng. Control*, 26(5), 277–282.

Guo, X., Dunne, M. C., and Black, J. A. (2004). "Modeling of pedestrian delays with pulsed vehicular traffic flow." *Transp. Sci.*, 38(1), 86–96.

Heydecker, B. G., and Dudgeon, I. W. (1987). "Calculation of signal settings to minimise delay at a junction." *Transp. Traffic Theory*, 27(1), 159–178.

Improta, G., and Cantarella, G. (1984). "Control system design for an individual signalized junction." *Transp. Res. Part B: Methodol.*, 18(2), 147–167.

Ishaque, M. M., and Noland, R. B. (2005). "Multimodal microsimulation of vehicle and pedestrian signal timings." *Trans. Res. Rec.*, 1939, 107–114.

Janos, M., and Furth, P. G. (2002). "Bus priority with highly interruptible traffic signal control: Simulation of San Juan's Avenida Ponce de Leon." *Transp. Res. Rec.*, 1811, 157–165.

Kattan, L., Acharjee, S., and Tay, R. (2009). "Pedestrian scramble operations: Pilot study in Calgary, Alberta, Canada." *Transp. Res. Rec.*, 2140, 79–84.

Khoo, H. L., Teoh, L. E., and Meng, Q. (2014). "A bi-objective optimization approach for exclusive bus lane selection and scheduling design." *Eng. Optim.*, 46(7), 987–1007.

Kim, J. T. (2010). "Triple-ring phase representation scheme for exclusive median bus lane signals." *Can. J. Civ. Eng.*, 37(8), 1117–1124.

Kim, T. J., and Suh, S. (1988). "Toward developing a national transportation planning model: A bilevel programming approach for Korea." *Ann. Reg. Sci.*, 22(S1), 65–80.

Kruszyna, M., Mackiewicz, P., and Szydlo, A. (2006). "Influence of pedestrians' entry process on pedestrian delays at signal-controlled crosswalks." *J. Transp. Eng.*, 10.1061/(ASCE)0733-947X(2006)132:11(855), 855–861.

Lee, J. Y. S., and Lam, W. H. K. (2008). "Simulating pedestrian movements at signalized crosswalks in Hong Kong." *Transp. Res. Part A: Policy Pract.*, 42(10), 1314–1325.

Li, Q., Wang, Z., Yang, J., and Wang, J. (2005). "Pedestrian delay estimation at signalized intersections in developing cities." *Transp. Res. Part A: Policy Pract.*, 39(1), 61–73.

Li, S. G., and Ju, Y. F. (2009). "Evaluation of bus-exclusive lanes." *IEEE Trans. Intell. Transp. Syst.*, 10(2), 236–245.

Lin, W. H. (2002). "Quantifying delay reduction to buses with signal priority treatment in mixed-mode operation." *Transp. Res. Rec.*, 1811, 100–106.

Liu, H. C., Han, K., Gayah, V. V., Friesz, T. L., and Yao, T. (2015). "Data-driven linear decision rule approach for distributionally robust optimization of on-line signal control." *Transp. Res. Part C: Emerging Technol.*, 59, 260–277.

Lu, G. X., Zhang, Y., and Noyce, D. A. (2011). "Intelligent traffic signal system for isolated intersections: Dynamic pedestrian accommodation." *Trans. Res. Rec.*, 2259, 96–111.

Ma, W. J., Head, K. L., and Feng, Y. (2014a). "Integrated optimization of transit priority operation at isolated intersections: A person-capacity-based approach." *Transp. Res. Part C: Emerging Technol.*, 40(1), 49–62.

Ma, W. J., Liao, D., Liu, Y., and Hong, K. L. (2015). "Optimization of pedestrian phase patterns and signal timings for isolated intersection." *Transp. Res. Part C: Emerging Technol.*, 58, 502–514.

Ma, W. J., Liu, Y., and Head, K. L. (2014b). "Optimization of pedestrian phase patterns at signalized intersections: A multi-objective approach." *J. Adv. Transp.*, 48(8), 1138–1152.

Ma, W. J., Liu, Y., Xie, H., and Yang, X. (2011). "Multiobjective optimization of signal timings for two-stage, midblock pedestrian crosswalk." *Trans. Res. Rec.*, 2264, 34–43.

Ma, W. J., Ni, W., Head, K. L., and Zhao, J. (2013). "Effective coordinated optimization model for transit priority control under arterial progression." *Trans. Res. Rec.*, 2356, 71–83.

Ma, W. J., Yang, X. G., and Liu, Y. (2010). "Development and evaluation of a coordinated and conditional bus priority approach." *Trans. Res. Rec.*, 2145, 49–58.

Mesbah, M., Sarvi, M., and Currie, G. (2011a). "Optimization of transit priority in the transportation network using a genetic algorithm." *IEEE Trans. Intell. Transp. Syst.*, 12(3), 908–919.

Mesbah, M., Sarvi, M., Ouveysi, I., and Currie, G. (2011b). "Optimization of transit priority in the transportation network using a decomposition methodology." *Transp. Res. Part C: Emerging Technol.*, 19(2), 363–373.

Messac, A. (2000). "From dubious construction of objective functions to the application of physical programming." *AIAA J.*, 38(1), 155–163.

Miandoabchi, E., Farahani, R. Z., and Szeto, W. Y. (2012). "Bi-objective bimodal urban road network design using hybrid metaheuristics." *Cent. Eur. J. Oper. Res.*, 20(4), 583–621.

NACTO (National Association of City Transportation Officials) (2016). *Transit street design guide*, New York.

Nagraj, R., and Vedagiri, P. (2013). "Modeling pedestrian delay and level of service at signalized intersection at signalized intersection crosswalks under mixed traffic conditions." *Trans. Res. Rec.*, 2394, 70–76.

Nakayama, H., Yun, Y., and Yoon, M. (2009). *Sequential approximate multiobjective optimization using computational intelligence*, Springer, Berlin.

Silcock, J. (1997). "Designing signal-controlled junctions for group-based operation." *Transp. Res. Part A: Policy Pract.*, 31(2), 157–173.

Skabardonis, A. (2000). "Control strategies for transit priority." *Trans. Res. Rec.*, 1727, 30–34.

Szeto, W. Y., and Lo, H. K. (2005). "Strategies for road network design over time: Robustness under uncertainty." *Transportmetrica*, 1(1), 47–63.

Tong, Y., Zhao, L., Li, L., and Zhang, Y. (2015). "Stochastic programming model for oversaturated intersection signal timing." *Transp. Res. Part C: Emerging Technol.*, 58, 474–486.

TRB (Transportation Research Board). (2010). *Highway capacity manual 2010*, Washington, DC.

TRB (Transportation Research Board). (2013). *Transit capacity and quality of service manual*, Washington, DC.

Virkler, M. R. (1998). "Pedestrian compliance effects on signal delay." *Trans. Res. Rec.*, 1636, 88–91.
VISSIM [Computer software]. PTV AG, Karlsruhe, Germany.
Wang, X., and Tian, Z. (2010). "Pedestrian delay at signalized intersections with a two-stage crossing design." *Trans. Res. Rec.*, 2173, 133–138.
Webster, F. V. (1958). *Traffic signal settings*, Her Majesty's Stationery Office, London.
Wei, D., Tian, H. L., and Tian, Z. (2015). "Vehicle delay estimation at unsignalised pedestrian crosswalks with probabilistic yielding behaviour." *Transportmetrica A: Transp. Sci.*, 11(2), 103–118.
Wong, C., and Wong, S. (2003a). "A lane-based optimization method for minimizing delay at isolated signal-controlled junctions." *J. Mathematical Modell. Algorithms*, 2(4), 379–406.
Wong, C., and Wong, S. (2003b). "Lane-based optimization of signal timings for isolated junctions." *Transp. Res. Part B: Methodological*, 37(1), 63–84.
Wong, C. K., and Heydecker, B. (2011). "Optimal allocation of turns to lanes at an isolated signal-controlled junction." *Transp. Res. Part B: Methodological*, 45(4), 667–681.
Xu, H. F., and Zheng, M. M. (2012). "Impact of bus-only lane location on the development and performance of the logic rule-based bus rapid transit signal priority." *J. Transp. Eng.*, 10.1061/(ASCE)TE.1943-5436.0000325, 293–314.
Yang, Z. Y., and Benekohal, R. F. (2011). "Use of genetic algorithm for phase optimization at intersections with minimization of vehicle and pedestrian delays." *Trans. Res. Rec.*, 2264, 54–64.
Yao, J., Shi, F., Zhou, Z., and Qin, J. (2012). "Combinatorial optimization of exclusive bus lanes and bus frequencies in multi-modal transportation network." *J. Transp. Eng.*, 10.1061/(ASCE)TE.1943-5436.0000475, 1422–1429.
Ye, X., Chen, J., Jiang, G., and Yan, X. (2015). "Modeling pedestrian level of service at signalized intersection crosswalks under mixed traffic conditions." *Trans. Res. Rec.*, 2512, 46–55.
Yin, Y. (2008). "Robust optimal traffic signal timing." *Transp. Res. Part B: Methodol.*, 42(10), 911–924.
Yu, B., Kong, L., Sun, Y., Yao, B. Z., and Gao, Z. Y. (2015). "A bi-level programming for bus lane network design." *Transp. Res. Part C: Emerging Technol.*, 55, 310–327.
Yu, C., Ma, W., Han, K., and Yang, X. (2017). "Optimization of vehicle and pedestrian signals at isolated intersections." *Transp. Res. Part B: Methodol.*, 98, 135–153.
Zhang, L., Yin, Y., and Lou, Y. (2010). "Robust signal timing for arterials under day-to-day demand variations." *Trans. Res. Rec.*, 2192, 156–166.
Zhao, J., Liu, Y., and Li, P. (2016). "A network enhancement model with integrated lane reorganization and traffic control strategies." *J. Adv. Transp.*, 50(6), 1090–1110.